

## Supplementary Information

### **A dual-biomimetic knitted fabric with manipulative structure and wettability for highly efficient fog harvesting**

Zhihua Yu<sup>a</sup>, Shuhui Li<sup>b</sup>, Mingming Liu<sup>a,\*</sup>, Ruofei Zhu<sup>a</sup>, Mengnan Yu<sup>a</sup>, Xiuli Dong<sup>a</sup>, Yaxin Sun<sup>a</sup> and Shaohai Fu<sup>a,\*</sup>

<sup>a</sup>Jiangsu Engineering Research Center for Digital Textile Inkjet Printing, Key Laboratory of Eco-Textile, Jiangnan University, Ministry of Education, Wuxi, Jiangsu 214122, China

<sup>b</sup>Wenzhou Institute, University of Chinese Academy of Sciences, Wenzhou 325011, PR China

---

*a. Jiangsu Engineering Research Center for Digital Textile Inkjet Printing, Key Laboratory of Eco-Textile, Jiangnan University, Ministry of Education, Wuxi, Jiangsu 214122, China.*

*b. Wenzhou Institute, University of Chinese Academy of Sciences, Wenzhou 325011, PR China.*

\* Corresponding authors.

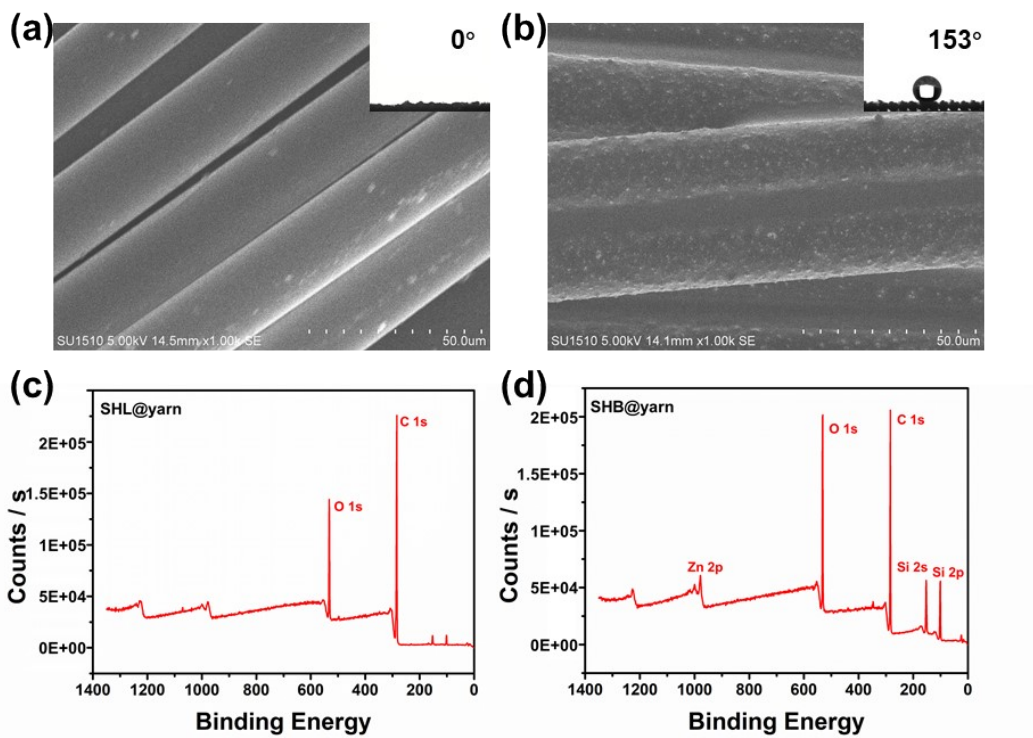


**Fig. S1** SEM and XPS of SHL yarns (a,c) and SHB yarns (b,d), insets are the WCA of

SHL

and

SHB

yarns.

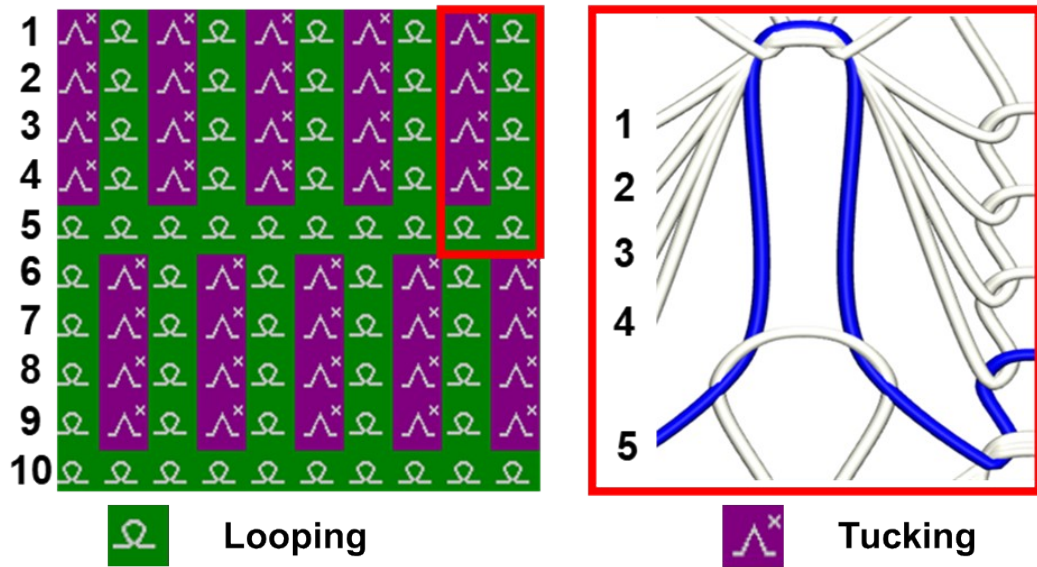


**Fig. S2** The drawing plan of SHL-SHB@TF. Each row represents a single yarn, and each column represents the shape of the yarn at that position. As indicated by red frame, a basic structure of SHL-SHB@TF costs 5 rows and 2 columns. A green cell and violet cell represent that the yarn at that position forms an elongated closed loop (Looping) and an unclosed V-shape loop (Tucking), respectively. By replacing the 5th yarn with a SHB yarn to obtain SHL-SHB@TF.

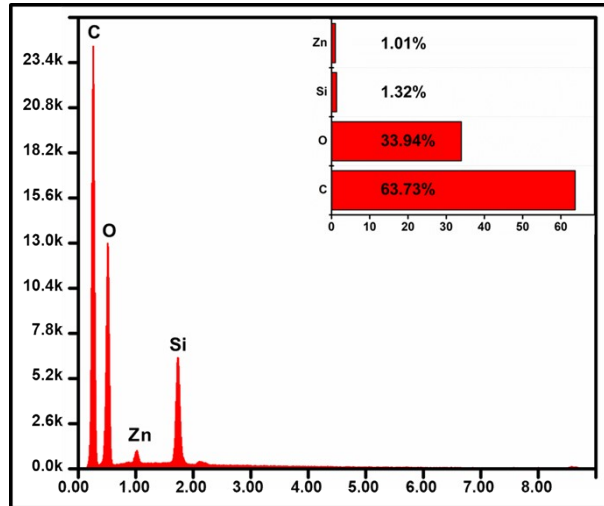


**Fig. S3** Atomic ratio of each element of SHL-SHB@TF.

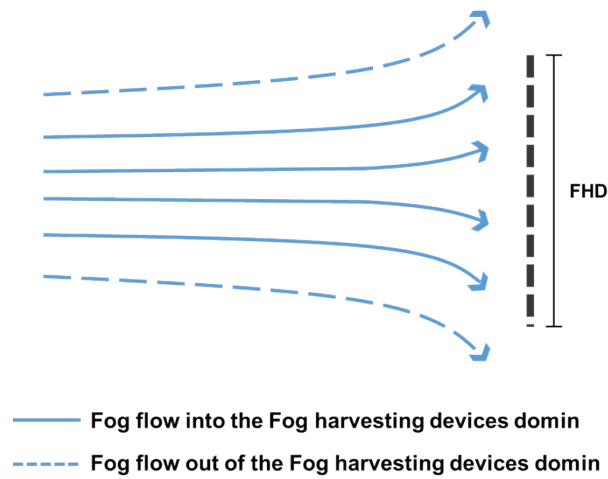


**Fig. S4** Illustration of aerodynamic deviation. When the fog flows to the FHD, it will be subjected to the resistance generated by the FHD, thereby causing it to deviation. The solid curves represent the fog flow which can flow into the FHD domain, and the dotted curves represent the fog flow which circumventing the mesh domain.

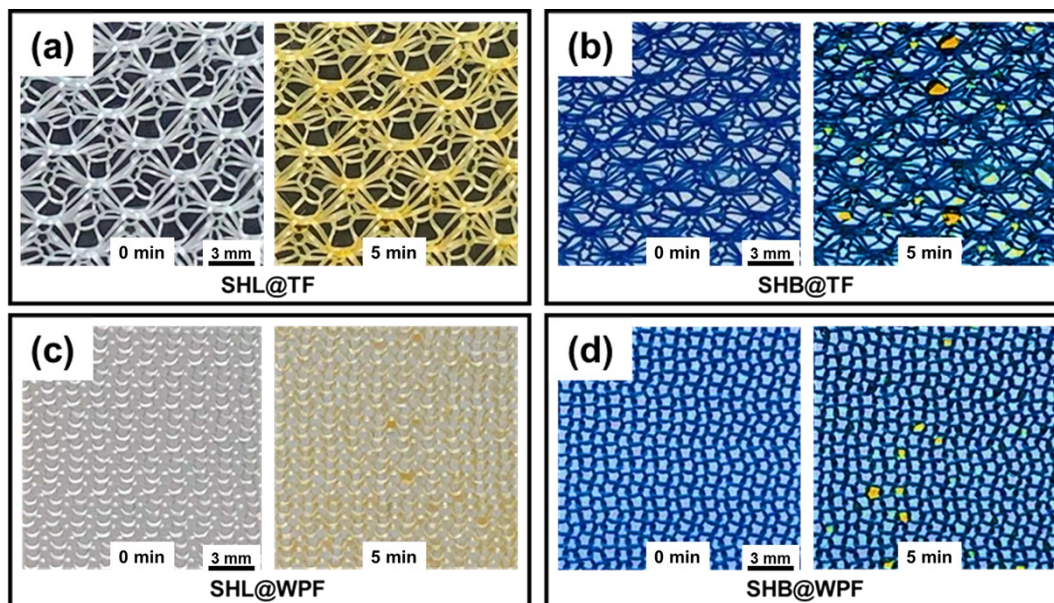


**Fig. S5** Fog capturing photos during 5 min of SHL@TF (a), SHB@TF (b), SHL@WPF (c) and SHB@WPF (d).

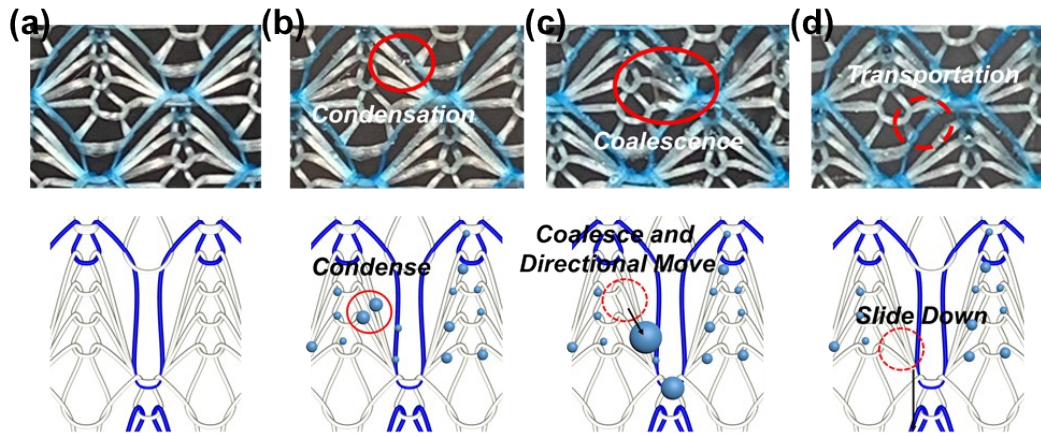


**Fig. S6** Fog harvesting process of SHL-SHB@TF, including fog droplets condense, coalescence, directional move and slide down.

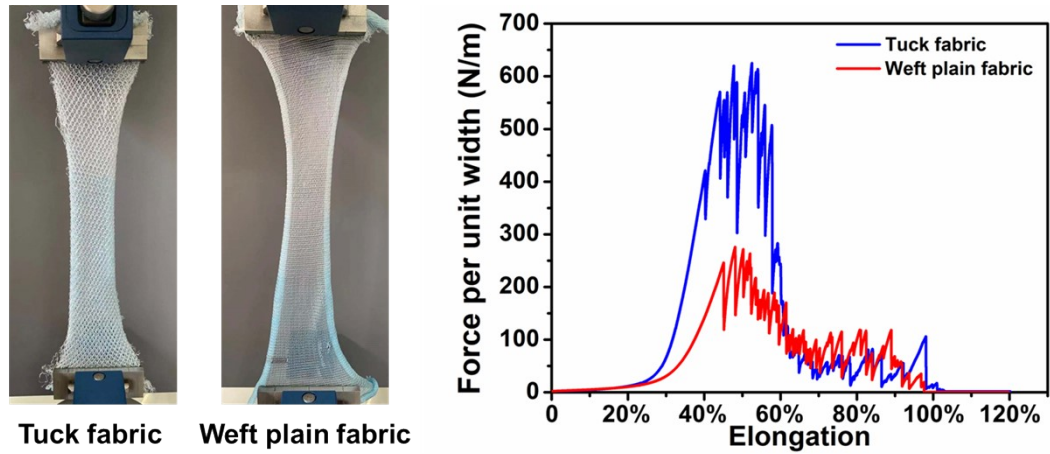


**Fig. S7** (a) Clamps and specimen mounted in the tensile test machine. This particular specimen is mounted with the transverse knitting direction oriented along the loading direction (vertical). (b) Force per unit width vs. elongation of Tuck fabric (blue) and Weft plain fabric (red).

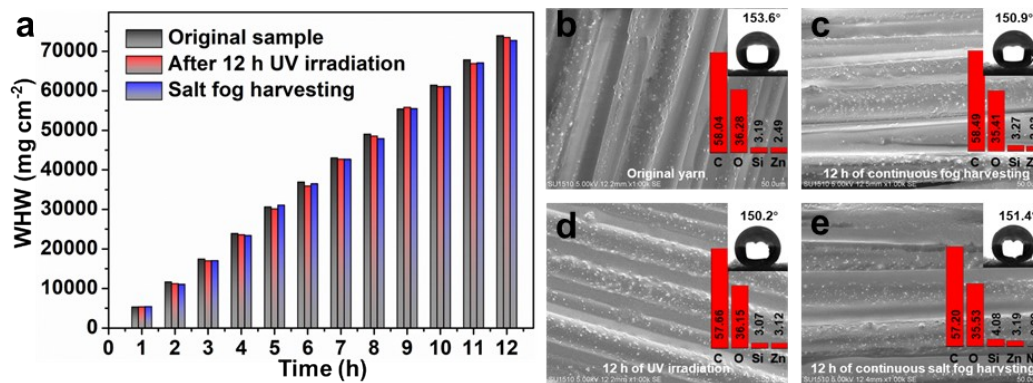


**Fig. S8** (a) Long-time continuous fog harvesting test (12 h) of original SHL-SHB@TF, SHL-SHB@TF after 12 h UV irradiation, and salt fog harvesting of SHL-SHB@TF. (b-d) the surface morphology, chemical composition and contact angle of original SHB yarn (b), SHB yarn after 12 h continuous fog harvesting (c), SHB yarn after 12 h UV irradiation (d) and SHB yarn after 12 h of salt fog harvesting (e).

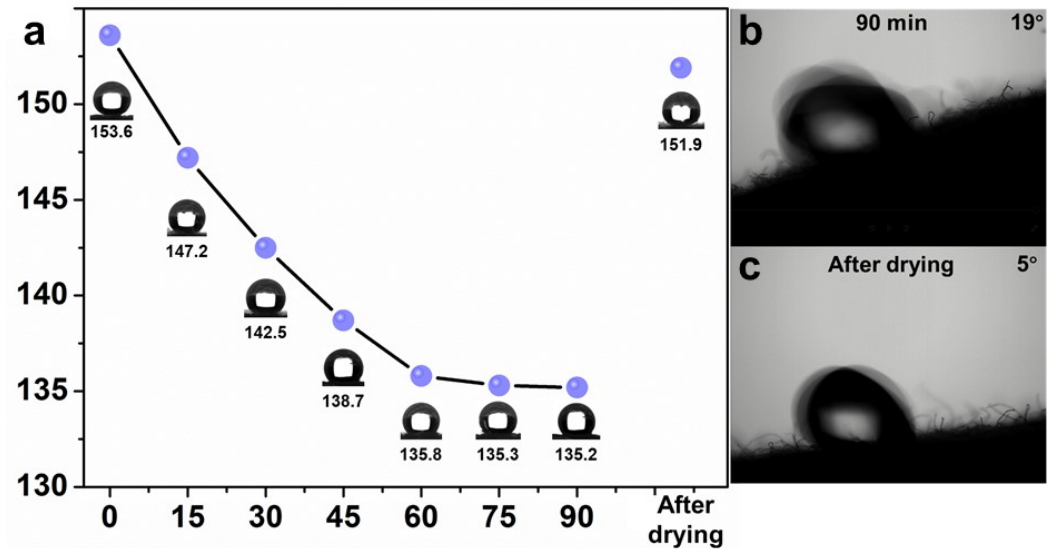


**Fig. S9** (a) The wettability of SHB yarn during fog harvesting process. The rolling angle of the SHB yarn in 90 min (b) and after drying (c).

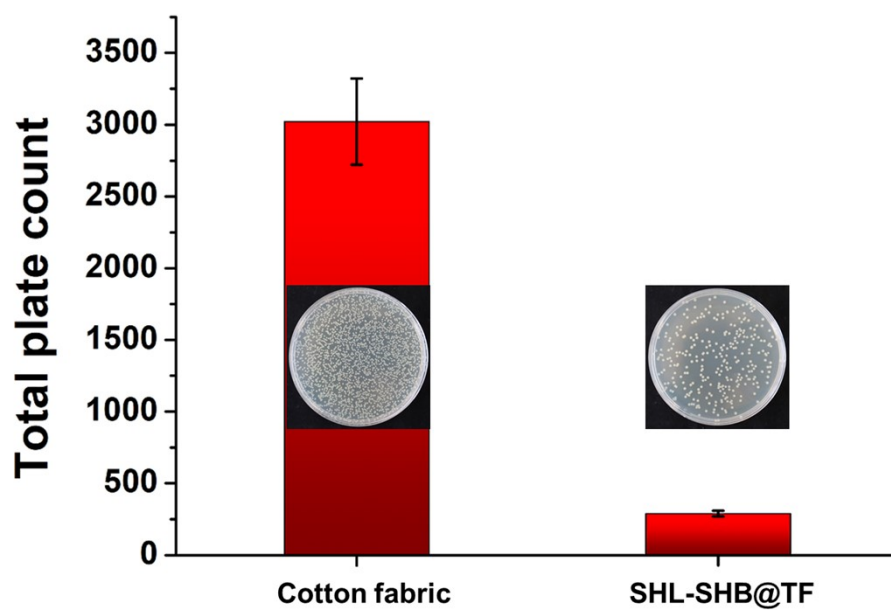


**Fig. S10** Antibacterial property of the cotton fabric and SHL-SHB@TF, insets are the optical photographs of bacteria attachment.

**Table S1.** A brief summary of the WHR about the mentioned 7 samples.

| Structure | Wettability    | Shadow coefficient | Position        | Water harvesting rate (mg h <sup>-1</sup> cm <sup>-2</sup> ) |
|-----------|----------------|--------------------|-----------------|--|
| WPF       | SHL            | 42.6%              | Downward        | 1866   |
| WPF       | SHB            | 42.6%              | Downward        | 2374   |
| WPF       | SHB-SHL        | 42.6%              | Downward        | 3874   |
| TF        | SHL            | 59.8%              | Downward        | 2700   |
| TF        | SHB            | 59.8%              | Downward        | 3203   |
| TF        | SHB-SHL        | 59.8%              | Downward        | 4240   |
| <b>TF</b> | <b>SHL-SHB</b> | <b>59.8%</b>       | <b>Downward</b> | <b>5424</b>  |
| TF        | SHL-SHB        | 59.8%              | Leftward        | 4492   |
| TF        | SHL-SHB        | 59.8%              | Upward          | 3820   |

**Table S2.** The comparison of the WHR and the cost performance of the fog harvesting devices.

| No | Fog harvesting device   | Fog flow rate<br>Distance<br>RH       | WHR                                      | Cost<br>(\$ m <sup>-2</sup> ) | Biggest defect  | Refs. |
|----|---|---------------------------------------|--|-------------------------------|---|-------|
| 1  | Artificial periodic roughness-gradient conical copper wire  | 1.8 m s <sup>-1</sup><br>/<br>90%     | 618 mg cm <sup>-2</sup> h <sup>-1</sup>  | ~ 79                          | Complex preparation process, high cost  | (1)   |
| 2  | A 600 mm <sup>2</sup> SHL bulgy surface with 120 SHB bulges on it   | 252 g h <sup>-1</sup><br>12 cm<br>85% | 430 mg cm <sup>-2</sup> h <sup>-1</sup>  | ~ 24                          | Complex preparation process and structure   | (2)   |
| 3  | The 3H fog harvesting surface fabricated by hot pressing of hydrophobic silica stripes on hydrophilic foam of melamine resin. | 120 cm s <sup>-1</sup><br>5 cm<br>/   | 2000 mg h <sup>-1</sup> cm <sup>-2</sup> | ~ 11                          | The roles of SHL wires and PDMS in the fog harvesting process are independent of each other | (3)   |
| 4  | The connection of SHL copper wires and SHB PDMS   | 50 cm s <sup>-1</sup><br>2 cm<br>/    | 1300 mg cm <sup>-2</sup> h <sup>-1</sup> | were                          | The roles of SHL wires and PDMS in the fog harvesting process are independent of each other | (4)   |

|    |   |   |  |      |   |      |
|----|---|---|--|------|---|------|
| 5  | Spraying micronanoparticles on SSM substrate and subsequent modification                        | 50 cm s <sup>-1</sup><br>5 cm<br>85~90% | 1700 mg h <sup>-1</sup> cm <sup>-2</sup>   | ~ 5  | The SHB-SHL pattern formed by particles was random  | (5)  |
| 6  | Three-layer sandwiched fog collector consisting of a SHL inner mesh and two SHB outer meshes    | 100 cm s <sup>-1</sup><br>6 cm<br>60%   | 3700 mg h <sup>-1</sup> cm <sup>-2</sup>   | ~ 15 | Two SHB outer meshes were difficult to capture fog droplets   | (6)  |
| 7  | A binary cooperative Janus fog collector integrated by SHL cotton absorbent and SHB copper mesh | 70 cm s <sup>-1</sup><br>5 cm<br>/      | 900 mg cm <sup>-2</sup> h <sup>-1</sup>    | ~ 4  | Captured fog water may be absorbed by SHL cotton and re- evaporation instead of harvested           | (7)  |
| 8  | Double-layer harp made of hydrophilic stainless steel wires                                     | Fog tower<br>/<br>/                     | 362.7 g min <sup>-1</sup> m <sup>-2</sup>  | ~ 5  | The captured droplets were difficult detached from hydrophilic stainless steel wires                | (8)  |
| 9  | Alloy net with gradient wettability   | 0.45 m s <sup>-1</sup><br>5 cm<br>90%   | 1050 mg cm <sup>-2</sup> h <sup>-1</sup>   | ~ 8  | Complex preparation process.  | (9)  |
| 10 | Patterned fabric through UV irradiation selective modification                                  | 10 cm s <sup>-1</sup><br>10 cm<br>90%   | 12,671 mg cm <sup>-2</sup> h <sup>-1</sup> | ~ 3  | During long-term application, the hydrophobic area may change to hydrophilic due to UV irradiation. | (10) |

|    |  |   |   |            |   |                  |
|----|--|---|---|------------|---|------------------|
| 11 | A superhydrophobic fabric surface with light-induced superhydrophilic bumps  | 200 mL h <sup>-1</sup><br>/<br>/                  | ~14 g   | ~ 3        | During long-term application, the hydrophobic area may change to hydrophilic due to UV irradiation.                                     | (11)             |
| 12 | Fabric made of 3D printed asymmetric fibers                                  | 195 L m <sup>-2</sup> day <sup>-1</sup><br>/<br>/ | 195 L m <sup>-2</sup> day <sup>-1</sup>       | ~ 30       | Lack of investigation of macroscopic physical structures  | (12)             |
| 13 | A patterned fabric woven from SHB and SHL yarn                               | 300 g h <sup>-1</sup><br>20 cm<br>90%             | 1432 .7 mg cm <sup>-2</sup> h <sup>-1</sup>   | ~ 1.5      | The impermeable structure were generated resistance to the fog flow, caused the fog flow to deviate, and reduced fog capture efficiency | (13)             |
| 14 | PVDF nanofibers directly deposit on Raschel mesh                             | 0.19 m·s <sup>-1</sup><br>6 cm<br>95% to 99%      | 64 mg cm <sup>-2</sup> h <sup>-1</sup>        | ~ 4        | The bonding force between the nanofiber and the mesh was poor   | (14)             |
| 15 | <b>Knited fabric with numerous conical channel and patterned wettability</b> | <b>300 g h<sup>-1</sup><br/>5 cm<br/>90%</b>      | <b>5424 mg cm<sup>-2</sup> h<sup>-1</sup></b> | <b>~ 1</b> | <b>/</b>  | <b>This work</b> |

References in the figure are shown below.

1. T. Xu et al. *ACS Nano*, 2016, **10**, 10681.
2. L. Zhong et al. *J. Colloid Interf. Sci.*, 2018, **525**, 234-242.

3. H. Bai et al. *J. Mater. Chem. A*, 2018, **6**, 20966.
4. L. Zhong et al. *Langmuir*, 2018, **34**, 15259-15267.
5. J. Feng et al. *Chem. Eng. J.*, 2020, **388**, 124283.
6. L. Wang et al. *J. Colloid Interf. Sci.*, 2021, **581**, 545–551.
7. M. Cao et al. *Small*, 2015, **11**, 4379-4384.
8. Jonathan B. Boreyko et al. *ACS Appl. Mater. Interfaces* 2020, **12**, 48124–48132.
9. Yongmei Zheng et al. *ACS Appl. Mater. Interfaces* 2020, **12**, 5065–5072.
10. Shaohai Fu et al. *ACS Appl. Mater. Interfaces* 2020, **12**, 50113–50125.
11. John H. Xin et al. *ACS Appl. Mater. Interfaces* 2016, **8**, 2950–2960.
12. Liqiu Wang et al. *Chem. Eng. J.*, 2021, **415**, 128944.
13. Y. Lai et al. *J. Mater. Sci. Technol.*, 2021, **61**, 85-92.
14. Urszula Stachewicz et al. *Sustain. Mater. Techno.*, 2020, **25**, e00191.

**Supplementary Movies:**

Movie S1. Capillary force of superhydrophilic yarns;

Movie S2. The rapid preparation process of samples based on fully automatic knitting machines;

Movie S3. Directional droplet transport in wedge-shaped tracks.

Movie S4. The moving behavior of droplets on different wettability samples;

Movie S5. The continuous fog harvesting process of SHL-SHB@TF.